Conductivity of the one-dimensional holographic *p*-wave superconductors in the presence of nonlinear electrodynamics

Mahya Mohammadi[1] and Ahmad Sheykhi[1,2,3,*]

[1]*Physics Department and Biruni Observatory, Shiraz University, Shiraz 71454, Iran*
[2] *Research Institute for Astronomy and Astrophysics of Maragha (RIAAM), P.O. Box 55134-441, Maragha, Iran*
[3]*Institut für Physik, Universität Oldenburg, Postfach 2503D-26111 Oldenburg, Germany*

We investigate analytically as well as numerically the effects of nonlinear Born-Infeld electrodynamics on the properties of $(1 + 1)$-dimensional holographic *p*-wave superconductors in the context of gauge-gravity duality. We consider the case in which the gauge and vector fields backreact on the background geometry. We apply the Sturm-Liouville eigenvalue problem for the analytical approach as well as the shooting method for the numerical calculations. In both methods, we find the relation between critical temperature T_c and chemical potential μ and show that both approaches are in good agreement with each other. We find that if one strengthens the effect of backreaction as well as nonlinearity, the critical temperature decreases, which means that the condensation is harder to form. We also explore the conductivity of the one-dimensional holographic *p*-wave superconductor for different values of *b* and T/T_c. We find that the real and imaginary parts of the conductivity have different behaviors in higher dimensions. The effects of different values of temperature are more apparent for larger values of the nonlinearity parameter. In addition, for the fixed value of T/T_c, by increasing the effect of nonlinearity, we observe larger values for a Drude-like peak in the real part of conductivity and a deeper minimum for the imaginary part.

I. INTRODUCTION

The idea of a holographic superconductor was proposed by Hartnoll *et al.* [1] by building a holographic *s*-wave superconductor in the background of four-dimensional Schwarzschild anti-de Sitter (AdS) black holes. The motivation was to shed light on the problem of high temperature superconductors. The most well-known theory of superconductors was proposed by Bardeen, Cooper, and Schrieffer (BCS); it can successfully explain the mechanism of low temperature superconductors. According to BCS theory, the condensation of pairs of electrons with antiparallel spins (Cooper pairs) interacts through the exchange of phonons into a bosonlike state [2]. To build the holographic superconductor, the correspondence between AdS spaces and conformal field theory (CFT) plays a crucial role [1,3]. According to the AdS/CFT dictionary, a strong coupling *d*-dimensional conformal field theory living on the boundary is equivalent to the weak coupling gravity theory in $(d + 1)$-dimensional AdS bulk, and each quantity in the bulk has a dual on the boundary [4–8]. In order to describe a superconductor at the boundary in a holographic scenario, we need a hairy

black hole in the bulk. More precisely, we need a hairy black hole (superconducting phase) for temperatures below the critical value and a black hole with no hair (normal phase or conductor phase) for upper values. During this process, the system undergoes the spontaneous $U(1)$ symmetry breaking. The condensation of a charged operator at the boundary corresponds to the emergence of the hair for black holes in the bulk. The quantum description of the hair for black holes is the gas of charged particles that have the same sign charge as the black hole. These are repelled away by the black hole and forbidden to escape to infinity due to the presence of the negative cosmological constant in the AdS bulk [9]. The holographic superconductor theory has received much attention in the past decade (see e.g., [10–32]). Moreover, holographic superconductors have also been widely explored in the regime of nonlinear electrodynamics (see e.g., [25–34]). There are several types of nonlinear electrodynamics such as the Born-Infeld (BI) [35], exponential [36], logarithmic [37], and power-Maxwell [27], the most famous being BI nonlinear electrodynamics which was first proposed for solving the divergency in the electrical field of the point particles [35,38–41]. Studies on the holographic superconductors have also generalized to other types such as *p*-wave superconductors. The *p*-wave superconductivity

*asheykhi@shirazu.ac.ir

is a phase of matter which occurs when the electrons are bounded with parallel spins by the exchange of electronic excitations with angular momentum $\ell = 1$ and condense in a triplet state. The terms odd-parity superconductivity, p-wave superconductivity, and triplet superconductivity are all equivalent [42]. Various models of holographic p-wave superconductors have been investigated. Holographic p-wave superconductors can be studied by condensation of a charged vector field in the bulk, which corresponds to the vector order parameter in the boundary [43,44]. This implies that the spin-1 order parameter can correspond to the condensation of a 2-form field on the gravity side [45]. In [46], this type of holographic superconductor is characterized by introducing a $SU(2)$ Yang-Mills gauge field in the bulk, in which one of the gauge degrees of freedom corresponds to the vector order parameter at the boundary. In addition, an alternative method to describe this kind of holographic superconductor emerges by adopting a complex vector field charged under a $U(1)$ gauge field, which is equivalent to a strongly coupled system involving a charged vector operator with a global $U(1)$ symmetry at the boundary [47]. For this type of holographic superconductor, by decreasing temperature below the critical value, the normal phase becomes unstable, and we observe the formation of vector hair, which corresponds to the superconducting phase. Other investigations on the holographic p-wave superconductors have been carried out in e.g., [47–53].

Furthermore, the $(1 + 1)$-dimensional holographic superconductors have been developed in the background of the BTZ black hole [8]. The BTZ black hole is the well-known solution of general relativity in $(2 + 1)$-dimensional spacetime which plays a crucial role in understanding the gravitational interaction in low dimensional spacetimes. In order to study the one-dimensional holographic superconductor, one may apply AdS_3/CFT_2 correspondence [54–58]. One-dimensional holographic s-wave and p-wave superconductors were analyzed both analytically and numerically from different points of view in e.g., [33,34,59–69]. It is worth noting that most investigations on the $(1 + 1)$-dimensional holographic p-wave superconductors are done in the framework of linear Maxwell electrodynamics. Therefore, it is fascinating to study the effects of nonlinearity in such a holographic superconductor. In the present work, we would like to extend the investigation on the one-dimensional holographic superconductor by considering the BI nonlinear electrodynamics when gauge and vector fields backreact on background geometry. It is worth noting that the $(1 + 1)$-dimensional holographic p-wave superconductor is located on the boundary of $(2 + 1)$-dimensional spacetime, while the gauge and the vector fields are defined in the $(2 + 1)$-dimensional BTZ black hole. It is well known that the electric field of a point charge in $(2 + 1)$ dimensions has

the form $E(r) = q/r$. Thus, there is still a divergency in the electric field at the location of the point charge ($r = 0$). However, taking the BI electrodynamics into account can remove this divergency as well. This is the main motivation for investigating the $(1 + 1)$-dimensional holographic p-wave superconductor in the presence of nonlinear BI electrodynamics.

We employ both analytical and numerical approaches. Our analytical study is based on the Sturm-Liouville eigenvalue problem, while the shooting method is used for the numerical calculations. Our aim is to find a relation between the critical temperature T_c and the chemical potential μ for different values of backreaction and nonlinear parameters. We also investigate the effects of nonlinearity on the real and imaginary parts of conductivity.

This article is organized as follows. In Sec. II we introduce the one-dimensional holographic p-wave superconductor. In Sec. III, we study condensation of the vector field both analytically and numerically. In Sec. IV, we calculate the critical exponent of this type of holographic superconductor analytically as well as numerically. In Sec. V, we explore the holographic conductivity for this model. Finally, in Sec. VI, we present a summary of our results and a discussion.

II. THE HOLOGRAPHIC P-WAVE MODEL

In a three-dimensional spacetime, the action of Einstein gravity in the presence of nonlinear BI electrodynamics and a negative cosmological constant can be written as

$$S = \frac{1}{2\kappa^2} \int d^3x \sqrt{-g} \mathcal{L}_G + \int d^3x \sqrt{-g} \mathcal{L}_m,$$

$$\mathcal{L}_G = R + \frac{2}{l^2},$$

$$\mathcal{L}_m = \mathcal{L}(\mathcal{F}) - \frac{1}{2}\rho_{\mu\nu}^{\dagger}\rho^{\mu\nu} - m^2\rho_{\mu}^{\dagger}\rho^{\mu} + iq\gamma\rho_{\mu}\rho_{\nu}^{\dagger}F^{\mu\nu}. \quad (1)$$

In the Lagrangian of the matter field, $\mathcal{L}_m$, the constants m and q are the mass and charge of the vector field ρ_{μ}, respectively. Here, $\kappa^2 = 8\pi G_3$ where G_3 is the three-dimensional Newtonian gravitation constant in the bulk. In addition, the metric determinant, Ricci scalar, and AdS radius are characterized by g, R, and l, respectively. Also, $F_{\mu\nu} = \nabla_\mu A_\nu - \nabla_\nu A_\mu$ is the strength of the Maxwell field, with A_μ as the vector potential. Considering $D_\mu = \nabla_\mu - iqA_\mu$ we can define $\rho_{\mu\nu} = D_\mu\rho_\nu - D_\nu\rho_\mu$. The last term in the matter Lagrangian, which represents a nonlinear interaction between ρ_μ and A_μ with γ the magnetic moment, can be ignored in the present work because we consider the case without an external magnetic field. The Lagrangian density of the BI nonlinear electrodynamics is given by $\mathcal{L}(\mathcal{F})$ and can be defined as

$$\mathcal{L}(\mathcal{F}) = \frac{1}{b}\left(1 - \sqrt{1 + \frac{b\mathcal{F}}{2}}\right), \qquad (2)$$

where b is the nonlinear parameter and $\mathcal{F} = F_{\mu\nu}F^{\mu\nu}$. When $b \to 0$, $\mathcal{L}(\mathcal{F})$ reduces to the standard Maxwell Lagrangian.

Varying the action (1) with respect to the metric $g_{\mu\nu}$, the gauge field A_μ, and the vector field ρ_μ yields the equations of motion for the gravitational and the bulk matter fields as

$$\frac{1}{2\kappa^2}\left[R_{\mu\nu} - g_{\mu\nu}\left(\frac{R}{2} + \frac{1}{l^2}\right)\right]$$
$$= -2F_{\mu\lambda}F_\nu{}^\lambda\mathcal{L}_\mathcal{F} + \frac{1}{2}\mathcal{L}_m g_{\mu\nu} + \frac{1}{2}[\rho^\dagger{}_{\mu\lambda}\rho_\nu^\lambda + m^2\rho^\dagger{}_\mu\rho_\nu$$
$$- i\gamma q F_\nu^\lambda(\rho_\mu\rho^\dagger{}_\lambda - \rho^\dagger{}_\mu\rho_\lambda) + \mu \leftrightarrow \nu], \qquad (3)$$

$$\nabla^\nu(-4\mathcal{L}_\mathcal{F}F_{\nu\mu})$$
$$= iq(\rho^\nu\rho^\dagger{}_{\nu\mu} - \rho^{\nu\dagger}\rho_{\nu\mu}) + iq\gamma\nabla^\nu(\rho_\nu\rho^\dagger{}_\mu - \rho^\dagger{}_\nu\rho_\mu), \qquad (4)$$

$$D^\nu\rho_{\nu\mu} - m^2\rho_\mu + iq\gamma\rho^\nu F_{\nu\mu} = 0, \qquad (5)$$

where $\mathcal{L}_\mathcal{F} = \partial\mathcal{L}/\partial\mathcal{F}$. In order to study the backreacted $(1+1)$-dimensional holographic p-wave superconductor in the presence of BI nonlinear electrodynamics, we consider the following ansatz for the metric and bulk fields:

$$ds^2 = -f(r)e^{-\chi(r)}dt^2 + \frac{dr^2}{f(r)} + r^2 dx^2, \qquad (6)$$

$$\rho_\nu dx^\nu = \rho_x(r)dx, \qquad A_\nu dx^\nu = \phi(r)dt, \qquad (7)$$

where the x component of the vector field ρ_x corresponds to the expectation value $\langle J_x \rangle$ which plays the role of the order parameter in the boundary theory. The Hawking temperature of the black hole is given by [34]

$$T = \frac{e^{-\chi(r_+)/2}f'(r_+)}{4\pi}. \qquad (8)$$

Substituting relations (6) and (7) in the field equations (3) and (4), we arrive at

$$f'(r) - \frac{2r}{l^2} + 2\kappa^2 r\left[\frac{1}{b\sqrt{1 - be^{\chi(r)}\phi'^2(r)}} - \frac{1}{b}\right.$$
$$\left. + \frac{q^2\rho_x^2(r)e^{\chi(r)}\phi^2(r)}{r^2 f(r)} + \frac{f(r)\rho_x'^2(r)}{r^2} + \frac{m^2\rho_x^2(r)}{r^2}\right] = 0, \qquad (9)$$

$$\chi'(r) + \frac{4\kappa^2}{r}\left[\frac{q^2\rho_x^2(r)e^{\chi(r)}\phi^2(r)}{f^2(r)} + \rho_x'^2(r)\right] = 0, \qquad (10)$$

$$\phi''(r) + \phi'(r)\left[\frac{\chi'(r)}{2} + \frac{1}{r} - \frac{be^{\chi(r)}\phi'^2(r)}{r}\right]$$
$$- \frac{2q^2\rho_x^2(r)\phi(r)}{r^2 f(r)}[1 - be^{\chi(r)}\phi'^2(r)]^{3/2} = 0, \qquad (11)$$

$$\rho_x''(r) + \rho_x'(r)\left[\frac{f'(r)}{f(r)} - \frac{\chi'(r)}{2} - \frac{1}{r}\right]$$
$$+ \rho_x(r)\left[\frac{q^2 e^{\chi(r)}\phi^2(r)}{f^2(r)} - \frac{m^2}{f(r)}\right] = 0. \qquad (12)$$

Here, the prime denotes the derivative with respect to r. In the presence of the nonlinear BI electrodynamics, Eqs. (12) and (10) do not change in comparison with the linear Maxwell case. In the limiting case where $b \to 0$, the equations of motion of the Maxwell field are reproduced [69]. If we consider the probe limit by setting $\kappa = 0$, the equations of motion (11) and (12) turn into the corresponding equations in [70]. There are scaling symmetries of the equations of motion (9)–(12) that we can use to set q and l equal to unity.

$$q \to q/a, \qquad \phi \to a\phi, \qquad \rho_x \to a\rho_x,$$
$$\kappa \to \kappa/a, \qquad b \to b/a^2, \qquad (13)$$

$$l \to al, \qquad r \to ar, \qquad q \to q/a,$$
$$b \to ba^2, \qquad m \to m/a. \qquad (14)$$

In addition, there is another symmetry which leaves the metric unchanged,

$$e^\chi \to a^2 e^\chi, \qquad t \to at, \qquad \phi \to a^{-1}\phi. \qquad (15)$$

Based on Eq. (15), the boundary value of χ is constant, so we can set $\chi = 0$. Considering μ and ρ as the chemical potential and charge density, the asymptotic behavior $(r \to \infty)$ of the field equations is given by

$$\phi(r) \sim \rho + \mu \ln(r), \qquad f(r) \sim r^2,$$
$$\chi(r) \to 0, \qquad \rho_x(r) \sim \frac{\rho_{x_-}}{r^{-m}} + \frac{\rho_{x_+}}{r^{+m}}. \qquad (16)$$

Taking the Breitenlohner-Freedman (BF) bound into account, $m^2 \geq 0$, ρ_{x_-} plays the role of the source and ρ_{x_+} is known as the x component of the expectation value of the order parameter $\langle J_x \rangle$ [71]. Hereafter, we set $m^2 = 1$. In the next sections, we investigate, analytically as well as numerically, the properties of one-dimensional backreacted holographic p-wave superconductors in the presence of BI nonlinear electrodynamics.

III. CONDENSATION OF VECTOR FIELD

Let us now investigate the relation between the critical temperature T_c and the chemical potential μ for holographic p-wave superconductors. In particular, we would like to explore the effects of backreaction as well as the nonlinearity parameter on the critical temperature.

A. Analytical approach

In order to follow our analytical studies, we apply the Sturm-Liouville eigenvalue problem and define $z = r_+/r$ as a new variable where $0 \leq z \leq 1$. Therefore, Eqs. (9)–(12) become

$$f'(z) + \frac{2r_+^2}{z^3} + \frac{2\kappa^2}{z}\left[-\rho_x^2(z) - \frac{e^{\chi(z)}\phi^2(z)\rho_x^2(z)}{f(z)}\right.$$
$$\left. - \frac{z^4 f(z)\rho_x'^2(z)}{r_+^2} + \frac{r_+^2}{bz^2}\left[1 - \frac{1}{\sqrt{1 - \frac{bz^4 e^{\chi(z)}\phi'^2(z)}{r_+^2}}}\right]\right] = 0,$$

(17)

$$\chi'(z) - 4\kappa^2\left[\frac{e^{\chi(z)}\phi^2(z)\rho_x^2(z)}{zf^2(z)} + \frac{z^3\rho_x'^2(z)}{r_+^2}\right] = 0, \quad (18)$$

$$\phi''(z) + \phi'(z)\left[\frac{1}{z} + \frac{\chi'(z)}{2} + \frac{bz^3 e^{\chi(z)}\phi'^2(z)}{r_+^2}\right]$$
$$- \frac{2\phi(z)\rho_x^2(z)}{z^2 f(z)}\left[1 - \frac{bz^4 e^{\chi(z)}\phi'^2(z)}{r_+^2}\right]^{3/2} = 0, \quad (19)$$

$$\rho_x''(z) + \rho_x'(z)\left[\frac{3}{z} - \frac{\chi'(z)}{2} + \frac{f'(z)}{f(z)}\right]$$
$$+ \rho_x(z)\left[\frac{r_+^2 e^{\chi(z)}\phi^2(z)}{z^4 f^2(z)} - \frac{r_+^2}{z^4 f(z)}\right] = 0. \quad (20)$$

Here, the prime indicates the derivative with respect to z. In the vicinity of the critical temperature, the expectation value of $\langle J_x \rangle$ is tiny, so we take it as an expansion parameter,

$$\epsilon \equiv \langle J_x \rangle.$$

We concentrate on the solutions for small values of the condensation parameter ϵ because near the critical temperature, we have $\epsilon \ll 1$. Therefore, we expand the functions in terms of the ϵ as

$$f \approx f_0 + \epsilon^2 f_2 + \epsilon^4 f_4 + \cdots,$$
$$\chi \approx \epsilon^2 \chi_2 + \epsilon^4 \chi_4 + \cdots,$$
$$\phi \approx \phi_0 + \epsilon^2 \phi_2 + \epsilon^4 \phi_4 + \cdots,$$
$$\rho_x \approx \epsilon\rho_{x_1} + \epsilon^3 \rho_{x_3} + \epsilon^5 \rho_{x_5} + \cdots.$$

Moreover, the chemical potential can be expressed as

$$\mu = \mu_0 + \epsilon^2 \delta\mu_2 + \cdots \rightarrow \epsilon \approx \left(\frac{\mu - \mu_0}{\delta\mu_2}\right)^{1/2}, \qquad \delta\mu_2 > 0.$$

Near the phase transition $\mu_c = \mu_0$, so the order parameter vanishes. In addition, the mean field value for the critical exponent $\beta = 1/2$ is obtained.

At zeroth order of ϵ, the equation for the gauge field (19) becomes

$$\phi''(z) + \frac{\phi'(z)}{z} + \frac{bz^3\phi'^3(z)}{r_+^2} = 0. \quad (21)$$

We can find the solution for this equation as follows:

$$\phi(z) = \lambda r_+ \log(z) - \frac{1}{4}b\lambda^3 r_+(z^2 - 1), \qquad \lambda = \frac{\mu}{r_+}. \quad (22)$$

Substituting solution (22) into Eq. (17), we arrive at

$$f'(z) + \frac{2r_+^2}{z^3} + \frac{2\kappa^2 r_+^2}{bz^3}\left(1 - \frac{1}{\sqrt{1 - \frac{bz^4\phi'^2(z)}{r_+^2}}}\right) = 0. \quad (23)$$

The solution for $f(z)$, at zeroth order of ϵ, can be obtained as

$$f(z) = \frac{r_+^2 g(z)}{z^2},$$
$$g(z) = 1 - z^2 + \kappa^2\lambda^2 z^2 \log(z) + \frac{1}{8}b\kappa^2\lambda^4 z^2 - \frac{1}{8}b\kappa^2\lambda^4 z^4.$$

(24)

Near the boundary, we can define the function $\rho_x(z)$ based on the trial function $F(z) = 1 - \alpha z^\varpi$ in which $\varpi \geq 2$ and satisfies the boundary conditions $F(0) = 1$ and $F'(0) = 0$,

$$\rho_x(z) = \frac{\langle J_x \rangle}{\sqrt{2}r_+^\Delta}z^\Delta F(z). \quad (25)$$

Inserting Eqs. (24) and (25) in Eq. (20), we arrive at

$$F''(z) + F'(z)\left[\frac{g'(z)}{g(z)} + \frac{2\Delta}{z} + \frac{1}{z}\right]$$

$$+ F(z)\left[\frac{\Delta g'(z)}{zg(z)} - \frac{1}{z^2 g(z)} + \frac{\Delta^2}{z^2}\right]$$

$$- \frac{F(z)\lambda^2 \log(z)}{2g^2(z)}[b\lambda^2 r_+(z^2 - 1) - 2\log(z)] = 0. \quad (26)$$

The Sturm-Liouville form of this equation is

$$[T(z)F'(z)]' + P(z)T(z)F(z) + \lambda^2 Q(z)T(z)F(z) = 0, \quad (27)$$

where

$$T(z) = z^{2\Delta+1}\left[(1 - z^2)\left(1 + \frac{b}{8}\kappa^2\lambda^4 z^2\right) + \kappa^2\lambda^2 z^2 \log(z)\right], \quad (28)$$

$$P(z) = \frac{\Delta}{z}\left(\frac{g'(z)}{g(z)} + \frac{\Delta}{z}\right) - \frac{1}{z^2 g(z)}, \quad (29)$$

$$Q(z) = \frac{\log(z)}{g^2(z)}\left[\log(z) + \frac{b}{2}\lambda^2 r_+(1 - z^2)\right]. \quad (30)$$

According to the Sturm-Liouville eigenvalue problem, we should minimize the following expression with respect to α.

$$\lambda^2 = \frac{\int_0^1 T(F'^2 - PF^2)dz}{\int_0^1 TQF^2 dz}. \quad (31)$$

The definition of the backreaction parameter, based on the iteration method, is [72]

$$\kappa_n = n\Delta\kappa, \quad n = 0, 1, 2, \ldots, \quad \Delta\kappa = \kappa_{n+1} - \kappa_n, \quad (32)$$

where we take $\Delta\kappa = 0.05$. In addition, we have

$$\kappa^2\lambda^2 = \kappa_n^2\lambda^2 = \kappa_n^2(\lambda^2|_{\kappa_{n-1}}) + O[(\Delta\kappa)^4],$$

$$\kappa_{-1} = 0, \quad \lambda^2|_{\kappa_{-1}} = 0, \quad (33)$$

$$b\lambda^2 = b(\lambda^2|_{b=0}) + \mathcal{O}(b^2). \quad (34)$$

Using Eqs. (8) and (9), the critical temperature, at zeroth order with respect to ϵ, is given by

$$T_c = \frac{f'(r_{+c})}{4\pi}$$

$$= \frac{r_{+c}}{4\pi}\left[2 - \kappa^2\lambda^2 + \frac{1}{4}b\kappa^2\lambda^4\right]$$

$$= \frac{1}{4\pi}\left(\frac{\mu}{\lambda}\right)\left[2 - \kappa_n^2(\lambda^2|_{\kappa_{n-1}}) + \frac{1}{4}b\kappa_n^2(\lambda^4|_{\kappa_{n-1}, b=0})\right]. \quad (35)$$

Considering three different forms of the trial function $F(z)$, the analytical results of T_c/μ affected by different values of backreaction and nonlinear parameters are listed in Tables I–III. Based on these results, the effects of increasing

TABLE I.   Analytical and numerical results of T_c/μ for different values of the backreaction and nonlinear parameters with the trial function $F(z) = 1 - \alpha z^2$.

	$b = 0$		$b = 0.04$		$b = 0.08$	
	Analytical	Numerical	Analytical	Numerical	Analytical	Numerical
$\kappa^2 = 0$	0.0478	0.0503	0.0416	0.0454	0.0343	0.0406
$\kappa^2 = 0.05$	0.0443	0.0410	0.0379	0.0366	0.0303	0.0324
$\kappa^2 = 0.1$	0.0424	0.0330	0.0361	0.0290	0.0281	0.0254
$\kappa^2 = 0.15$	0.0394	0.0260	0.0331	0.0226	0.0248	0.0195
$\kappa^2 = 0.2$	0.0353	0.0201	0.0291	0.0172	0.0205	0.0146
$\kappa^2 = 0.25$	0.0302	0.0152	0.0241	0.0127	0.0153	0.0106

TABLE II.   Analytical and numerical results of T_c/μ for different values of the backreaction and nonlinear parameters with $F(z) = 1 - \alpha z^3$.

	$b = 0$		$b = 0.04$		$b = 0.08$	
	Analytical	Numerical	Analytical	Numerical	Analytical	Numerical
$\kappa^2 = 0$	0.0466	0.0503	0.0400	0.0454	0.0320	0.0406
$\kappa^2 = 0.05$	0.0397	0.0410	0.0347	0.0366	0.0243	0.0324
$\kappa^2 = 0.1$	0.0375	0.0330	0.0328	0.0290	0.0215	0.0254
$\kappa^2 = 0.15$	0.0342	0.0260	0.0298	0.0226	0.0178	0.0195
$\kappa^2 = 0.2$	0.0296	0.0201	0.0258	0.0172	0.0132	0.0146
$\kappa^2 = 0.25$	0.0238	0.0152	0.0208	0.0127	0.0083	0.0106

TABLE III. Analytical and numerical results of T_c/μ for different values of the backreaction and nonlinear parameters with $F(z) = 1 - \alpha z^4$.

	$b = 0$		$b = 0.04$		$b = 0.08$	
	Analytical	Numerical	Analytical	Numerical	Analytical	Numerical
$\kappa^2 = 0$	0.0457	0.0503	0.0387	0.0454	0.0303	0.0406
$\kappa^2 = 0.05$	0.0379	0.0410	0.0328	0.0366	0.0205	0.0324
$\kappa^2 = 0.1$	0.0356	0.0330	0.0308	0.0290	0.0171	0.0254
$\kappa^2 = 0.15$	0.0321	0.0260	0.0278	0.0226	0.0131	0.0195
$\kappa^2 = 0.2$	0.0274	0.0201	0.0236	0.0172	0.0084	0.0146
$\kappa^2 = 0.25$	0.0214	0.0152	0.0186	0.0127	0.0039	0.0106

the backreaction parameter κ for a fixed value of the nonlinear parameter b are the same as increasing the nonlinear parameter for a fixed value of κ. In other words, in both cases, the value of T_c/μ decreases by increasing the backreaction or nonlinear parameters. Thus, the presence of backreaction and BI nonlinear electrodynamics makes it harder for the vector hair to form. In addition, for the case with $b = 0$, the results of [69] for T_c/μ are reproduced.

B. Numerical solution

To find the numerical solution for the $(1 + 1)$-dimensional holographic p-wave superconductor in the presence of backreaction and BI nonlinear electrodynamics, we employ the shooting method. For this purpose, we need to know the behavior of the equations of motion (18) and (19), both at the horizon and the boundary. We use the fact that $\phi(z = 1) = 0$; otherwise the norm of the gauge field A_μ will be ill defined at the horizon where $f(z = 1) = 0$. By using these conditions, we can expand the metric functions and vector field, around $z = 1$, as

$$f(z) = f_1(1 - z) + f_2(1 - z)^2 + \cdots, \quad (36)$$

$$\chi(z) = \chi_0 + \chi_1(1 - z) + \chi_2(1 - z)^2 + \cdots, \quad (37)$$

$$\phi(z) = \phi_1(1 - z) + \phi_2(1 - z)^2 + \cdots, \quad (38)$$

$$\rho_x(z) = \rho_{x_0} + \rho_{x_1}(1 - z) + \rho_{x_2}(1 - z)^2 + \cdots. \quad (39)$$

The higher orders will be disregarded because, in the vicinity of horizon, $(1 - z)^n$ is very small and can be neglected. In this method, we can write all coefficients in terms of ϕ_1, ρ_{x_0}, and χ_0. By varying these three parameters at the horizon, we try to gain the desirable state $\rho_{x_-}(\infty) = \chi(\infty) = 0$. In addition, we can set $r_+ = 1$ by virtue of the equations of motion's symmetry:

$$r \to ar, \qquad f \to a^2 f, \qquad \phi \to a\phi.$$

Consequently, the numerical values of T_c/μ for different values of backreaction and nonlinearity parameters are achieved. In order to show that there is a good agreement between analytical and numerical results, we present the numerical results in Tables I–III, too. However, we observe differences in the results in some cases, which originate from the fact that in order to solve the analytical solution, we use some simplifications. One may argue that these disagreements could be solved by considering the polynomial in the form of $F(z) = 1 - \alpha z^2 - \beta z^3 - \gamma z^4$, as the trial function. However, in this case one faces difficulties to achieve the solutions for larger values of the BI and backreaction parameters. Indeed, in this case, besides finding the parameter α, we have to find the β and γ parameters. Actually, the analytical method in holographic p-wave superconductors is very difficult. And for this reason, most studies on the holographic p-wave superconductors have been carried out numerically. In addition, the investigation of one-dimensional holographic

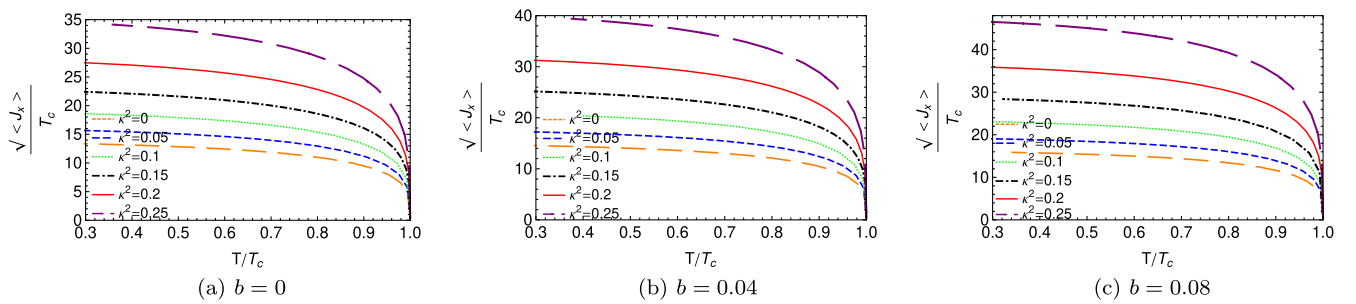(a) $b = 0$ (b) $b = 0.04$ (c) $b = 0.08$

FIG. 1. The behavior of the condensation parameter as a function of temperature for different values of backreaction.
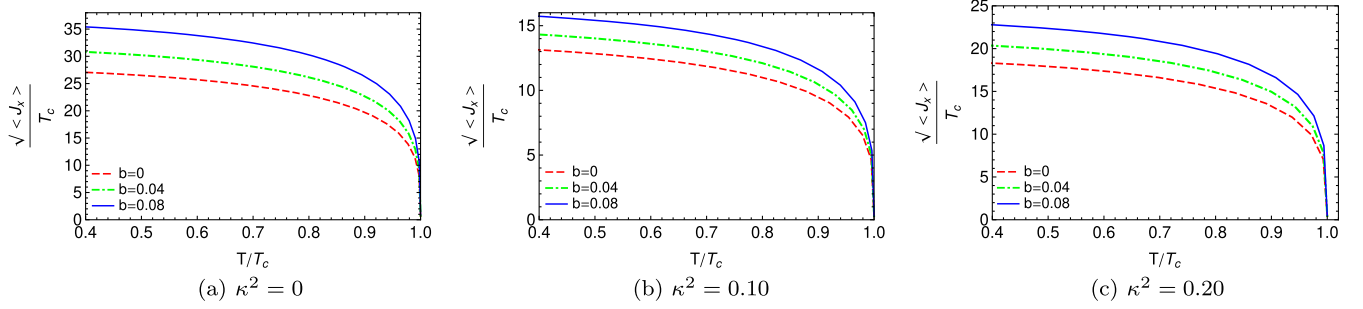
FIG. 2. Plot of the condensation as a function of temperature with $m^2 = 1$ for different values of the nonlinearity parameter b.

superconductors in the background of three-dimensional BTZ black holes is a difficult problem due to the logarithmic behavior of the gauge field ϕ. Overall, the shooting method's results follow the same trend as the results of the Sturm-Liouville method, namely, by increasing the strength of backreaction as well as the nonlinearity parameters for each form of the trial function $F(z)$. Indeed, increasing the values of the backreaction and nonlinear parameters makes it much harder to form the condensation. In addition, for $b = 0$, the numerical values of [69] are regained. Figures 1 and 2 show, respectively, the behavior of condensation as a function of temperature for different values of backreaction and nonlinear parameters. Based on these figures, the condensation gap increases for larger values of the backreaction and nonlinearity parameters, while the other one is fixed. This implies that it is harder to form a holographic p-wave superconductor in the presence of backreaction and BI nonlinear parameters.

IV. CRITICAL EXPONENTS

In this section, we calculate the expectation value of $\langle J_x \rangle$ in the vicinity of the critical temperature T_c for the one-dimensional holographic p-wave superconductor developed in a BTZ black hole background, when the gauge and vector fields backreact on the background geometry in the presence of BI nonlinear electrodynamics. Again, we perform our calculations both analytically and numerically.

A. Analytical study

To follow the analytical approach, we consider the behavior of the gauge field A_μ near the critical temperature. Since the condensation in the vicinity of the critical temperature is nonzero, we expect to have an extra term in the consequent equation compared to the field equation (21) in the previous section. Thus, Eq. (19) becomes

$$\phi''(z) + \frac{\phi'(z)}{z} + \frac{bz^3\phi'3(z)}{r_+^2}$$
$$- \frac{2\phi(z)\rho_x^2(z)}{z^2 f(z)}\left(1 - \frac{bz^4}{r_+^2}\phi'^2(z)\right)^{3/2} = 0. \quad (40)$$

Substituting Eqs. (24) and (25) in the above expression, we get

$$\phi''(z) + \frac{\phi'(z)}{z} + \frac{bz^3\phi'^3(z)}{r_+^2} = \frac{\langle J_x \rangle^2}{r_+^4}\phi(z)\Xi(z), \quad (41)$$

where

$$\Xi(z) = \frac{z^2 F^2(z)}{g(z)}\left(1 - \frac{3bz^4\phi'^2(z)}{2r_+^2}\right). \quad (42)$$

In order to find the solution of Eq. (41), we note that near the critical temperature, $T \simeq T_c$, the value of $\langle J_x \rangle^2/r_+^4$ is small, so we may write the solution in the form

$$\frac{\phi(z)}{r_+} = \lambda \log(z) - \frac{1}{4}b\lambda^3(z^2 - 1) + \frac{\langle J_x \rangle^2}{r_+^4}\eta(z). \quad (43)$$

At the horizon $\phi(z = 1) = 0$, we have $\eta(1) = 0$. Substituting Eq. (43) in Eq. (41), we arrive at

$$\eta''(z) + \frac{\eta'(z)}{z} + 3bz\lambda^2\eta'(z)$$
$$= \frac{\lambda z^2 F^2(z)}{g(z)}\left[\log(z) - \frac{1}{4}b\lambda^2(z^2 - 1) - \frac{3}{2}b\lambda^2 z^2\log(z)\right]. \quad (44)$$

Multiplying both sides of Eq. (44) by the factor $ze^{\frac{3}{2}b\lambda^2 z^2}$, we get

$$\int_0^1 d(ze^{\frac{3}{2}b\lambda^2 z^2}\eta'(z)) = e^{\frac{3b\lambda^2}{2}}\eta'(1) = \lambda\mathcal{A}, \quad (45)$$

where

$$\mathcal{A} = \int_0^1 \frac{z^3}{g(z)}F^2(z)e^{\frac{3}{2}b\lambda^2 z^2}\left[\log(z) - \frac{1}{4}b\lambda^2(z^2 - 1)\right.$$
$$\left. - \frac{3}{2}b\lambda^2 z^2\log(z)\right]dz. \quad (46)$$

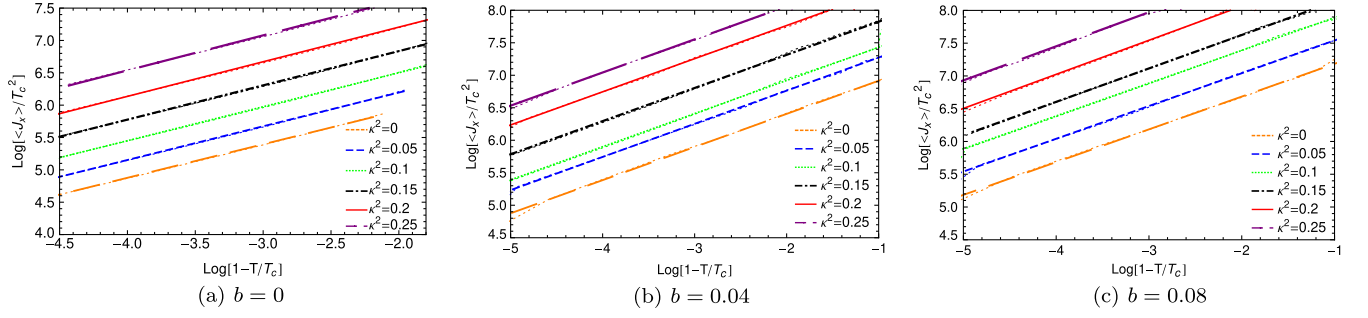Now, we use the coordinate transformation $z \to Z + 1$ in Eq. (22). Considering the fact that the first term on the rhs

FIG. 3. The behavior of $\log\langle J_x\rangle/T_c^2$ as a function of $\log(1 - T/T_c)$ with a slope of $1/2$ for different values of backreaction parameters.

of Eq. (43) is the solution of $\phi(z)$ at the critical point, and the second term is a correction term, we have

$$\frac{\rho}{r_+} + \frac{\mu}{r_+}\log(1+Z) = \frac{\mu}{r_{+c}}\log(1+Z)$$
$$- \frac{1}{4}b\left(\frac{\mu}{r_{+c}}\right)^3[(1+Z)^2 - 1] + \frac{\langle J_x\rangle^2}{r_{+c}^4}\eta(1+Z). \quad (47)$$

Then, by expanding the resulting equation around $Z = 0$, we find

$$\frac{\rho}{r_+} + \frac{\mu}{r_+}\left(Z - \frac{Z^2}{2} + \cdots\right)$$
$$= \frac{\mu}{r_{+c}}\left(Z - \frac{Z^2}{2} + \cdots\right) - \frac{1}{4}b\left(\frac{\mu}{r_{+c}}\right)^3[(1+Z)^2 - 1]$$
$$+ \frac{\langle J_x\rangle^2}{r_{+c}^4}(\eta(1) + Z\eta'(1) + \cdots). \quad (48)$$

Comparing the coefficients Z on both sides of Eq. (48) and using Eq. (45), we find

$$\frac{\mu}{r_+} = \frac{\mu}{r_{+c}}\left(1 + \frac{\langle J_x\rangle^2}{r_{+c}^4}\mathcal{A}e^{-\frac{3}{2}b\lambda^2}\right). \quad (49)$$

Near the critical point, we have $T \sim T_c$, and thus using relation (35), we can find r_+ as

$$r_+ = \frac{4\pi T}{(2 - \kappa^2\lambda^2 + \frac{1}{4}b\kappa^2\lambda^4)}. \quad (50)$$

Inserting Eqs. (35) and (50) in Eq. (49) and taking the absolute values of the resulting equation, we arrive at

$$\langle J_x\rangle = \gamma T_c^2\sqrt{1 - \frac{T}{T_c}}, \quad (51)$$

where

$$\gamma = \frac{1}{\sqrt{|\mathcal{A}|}}\left(\frac{4\pi}{2 - \kappa^2\lambda^2 + \frac{1}{4}b\kappa^2\lambda^4}\right)^2 e^{\frac{3}{4}b\lambda^2}. \quad (52)$$

According to this equation, the critical exponent $\beta = 1/2$ is in good agreement with the mean field theory. We are faced with the second order phase transition for all values of the backreaction and nonlinear parameters because the value of β is independent of the effect of backreaction and nonlinearity. In addition, Eq. (52) for $b \to 0$ becomes the equivalent equation in [69].

B. Numerical approach

Using the results of the analytical solution for the condensation in the vicinity of the critical temperature [i.e., Eq. (51)], we have

$$\log\left(\frac{\langle J_x\rangle}{T_c^2}\right) = \log(\gamma) + \frac{1}{2}\log\left(1 - \frac{T}{T_c}\right). \quad (53)$$

Figures 3 and 4 give information about the behavior of $\log(\frac{\langle J_x\rangle}{T_c^2})$ as a function of $\log\left(1 - \frac{T}{T_c}\right)$ in the presence of
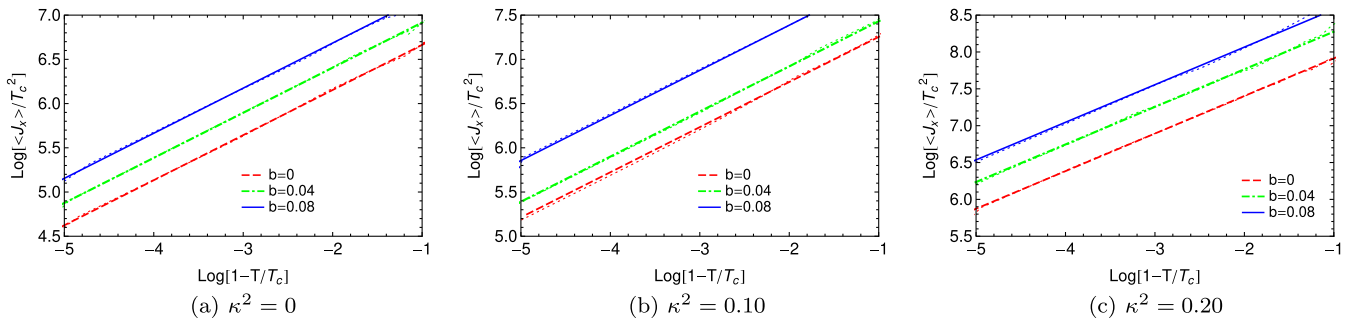

FIG. 4. The behavior of $\log\langle J_x\rangle/T_c^2$ as a function of $\log(1 - T/T_c)$ with a slope of $1/2$ for different values of nonlinearity parameters.

backreaction and BI nonlinear parameters. The slope of curves is 1/2, which is in agreement with the analytical approach. In addition, both methods follow the mean field theory, and the second order phase transition occurs.

V. CONDUCTIVITY

In this section, we obtain the electrical conductivity as a function of frequency for the one-dimensional holographic p-wave superconductors in the presence of backreaction and BI nonlinear electrodynamics by applying appropriate electromagnetic perturbations of A_x and g_{tx} on the black hole background. Based on the AdS/CFT correspondence, these perturbations in the bulk are dual to the boundary electric current. If we consider σ_{ij} and J_i as the electric conductivity and external electric field, according to the Ohm's law we have

$$\sigma_{ij} = \frac{J_i}{E_j}. \tag{54}$$

In order to calculate the conductivity in the x direction, we need to add the following perturbational terms in the bulk gauge potential and metric:

$$\delta A_x = A_x(r)e^{-i\omega t}, \qquad \delta g_{tx} = g_{tx}(r)e^{-i\omega t}. \tag{55}$$

Using Eq. (55), the linearized form of the x component of the electromagnetic equation (4) becomes

$$A''_x(r) + A'_x(r)\left[\frac{f'(r)}{f(r)} - \frac{\chi'(r)}{2} - \frac{1}{r} + \frac{2b\rho_x^2(r)e^{\chi(r)}\phi(r)\phi'(r)}{r^2 f(r)}\right.$$
$$\left. \times \sqrt{1 - be^{\chi(r)}\phi'^2(r)} - \frac{be^{\chi(r)}\phi'^2(r)}{r}\right] + A_x(r)\frac{\omega^2 e^{\chi(r)}}{f^2(r)}$$
$$+ \frac{e^{\chi(r)}\phi'(r)}{f(r)}\left[g'_{tx}(r) - \frac{2g_{tx}(r)}{r}\right]$$
$$+ \frac{2\rho_x^2(r)e^{\chi(r)}\phi(r)}{r^2 f^2(r)}g_{tx}(r)\sqrt{1 - be^{\chi(r)}\phi'^2(r)} = 0. \tag{56}$$

Also, using $(tt), (xx), (tx), (xt), (xr)$ components of the Einstein equations and after some simplification, we arrive at

$$\frac{1}{2\kappa^2}\left[g'_{tx}(r) - \frac{2g_{tx}(r)}{r}\right] + \frac{A_x(r)\phi'(r)}{\sqrt{1 - be^{\chi(r)}\phi'^2(r)}} = 0, \tag{57}$$

$$\frac{2}{r^2}A_x(r)\rho_x^2(r) + \frac{2\rho_x^2(r)e^{\chi(r)}\phi(r)}{r^2 f(r)}g_{tx}(r) = 0. \tag{58}$$

Substituting Eqs. (57) and (58) in Eq. (56), we obtain the linearized equation for the gauge field A_x,

$$A''_x(r) + A'_x(r)\left[\frac{f'(r)}{f(r)} - \frac{\chi'(r)}{2} - \frac{1}{r} + \frac{2b\rho_x^2(r)e^{\chi(r)}\phi(r)\phi'(r)}{r^2 f(r)}\right.$$
$$\left. \times \sqrt{1 - be^{\chi(r)}\phi'^2(r)} - \frac{be^{\chi(r)}\phi'^2(r)}{r}\right]$$
$$+ A_x(r)\left[\frac{\omega^2 e^{\chi(r)}}{f^2(r)} - \frac{2\rho_x^2(r)}{r^2 f(r)}\sqrt{1 - be^{\chi(r)}\phi'^2(r)}\right.$$
$$\left. - \frac{2\kappa^2 e^{\chi(r)}\phi'^2(r)}{f(r)\sqrt{1 - be^{\chi(r)}\phi'^2(r)}}\right] = 0. \tag{59}$$

Let us note that, of course, investigating the effects of nonlinearity as well as the backreaction parameters on the conductivity is a worthy task. However, in order to compute the conductivity in the holographic approach in the presence of nonlinear and backreaction parameters, we need to use the component of the gauge field as well as the metric. This extra component makes the calculations too difficult, and we are faced with difficulty in numerical solutions for the cases with nonzero values of backreaction. Therefore, for simplicity, in what follows, we consider only the probe limit by setting $g_{tx}(r) = 0 = \chi(r)$ in the presence of BI nonlinear electrodynamics. Thus, in the absence of backreaction, Eq. (56) can be written as

$$A''_x(r) + A'_x(r)\left[\frac{f'(r)}{f(r)} - \frac{1}{r} + \frac{2b\rho_x^2(r)\phi(r)\phi'(r)}{r^2 f(r)}\right.$$
$$\left. \times \sqrt{1 - b\phi'^2(r)} - \frac{b\phi'^2(r)}{r}\right] + \frac{\omega^2 A_x(r)}{f^2(r)} = 0, \tag{60}$$

where it admits the asymptotic solution in the following form:

$$A_x = A_x^{(0)} + A_x^{(1)}\log\left(\frac{1}{r}\right). \tag{61}$$

Based on the AdS/CFT dictionary, $A_x^{(0)}$ plays the role of the source in the dual theory, while $A_x^{(1)}$ gives the expectation value of the dual current. For the boundary current, we have
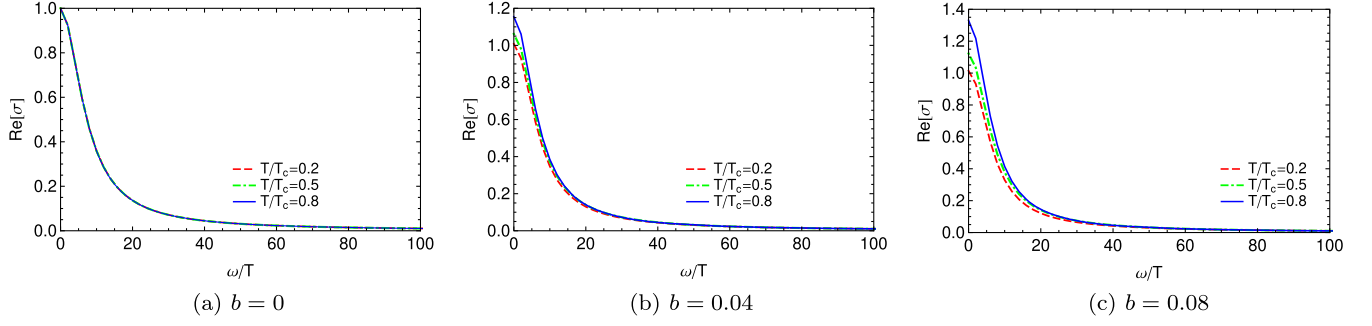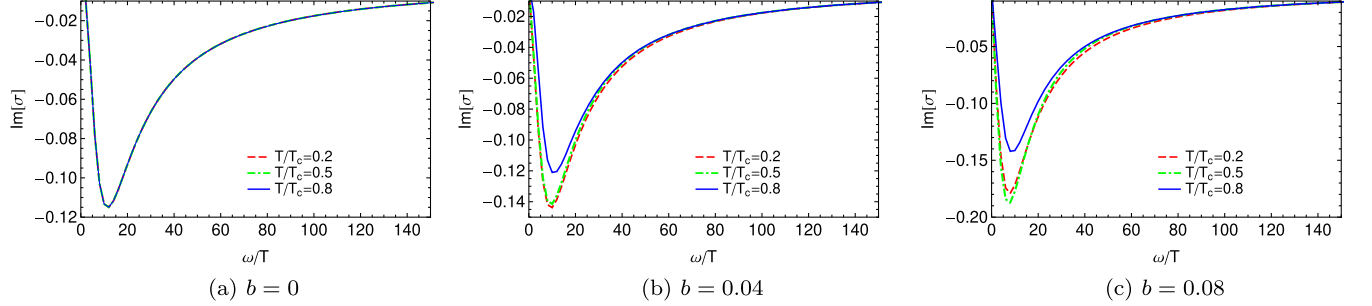
$$J = \frac{\delta S_{\text{bulk}}}{\delta A^{(0)}} = \frac{\delta S_{\text{o.s}}}{\delta A^{(0)}} = \frac{\partial(\sqrt{-g}\mathcal{L}_m)}{\partial A'_x}\bigg|r \to \infty, \tag{62}$$

where

$$S_{\text{o.s.}} = \int_{r_+}^{\infty} dr \int d^2 x \sqrt{-g}\mathcal{L}_m. \tag{63}$$

Integrating by parts and using Eq. (60), we get

$$S_{\text{o.s.}} = \int d^2 x \frac{f(r)A_x(r)A'_x(r)}{2r(1 - b\phi'^2(r))}. \tag{64}$$

FIG. 5.   The behavior of the real part of conductivity as a function of ω/T for different values of temperature in the case $\kappa^2 = 0$.

FIG. 6.   The behavior of the imaginary part of the conductivity as a function of ω/T for different values of temperature in the case $\kappa^2 = 0$.

Using the asymptotic behavior of $\phi(r)$, $f(r)$, and $A_x(r)$ given by Eqs. (16) and (61), we can calculate J_x. So, the electrical conductivity based on Eq. (54) is

$$\sigma(\omega) = \frac{J_x}{E_x} = -\frac{iA_x^{(1)}}{\omega A_x^{(0)}} = -\frac{izA_x'(z)}{\omega[A_x(z) - zA_x'(z)\log(z)]}, \quad (65)$$

where

$$E_x = -\partial_t \delta A_x. \quad (66)$$

Following the analytical approach to calculate conductivity seems difficult; thus we apply the numerical method. In order to do that, we consider the ingoing wave boundary condition in the vicinity of the horizon for $A_x(r)$ as follows:

$$A_x(r) = f(r)^{\frac{-i\omega}{4\pi T}}[1 + a(1-r) + b(1-r) + \cdots]. \quad (67)$$

In the above equation, T is the Hawking temperature, which in the probe limit $T = r_+/(2\pi)$, because in this case $f(r) = r^2 - 1$. Furthermore, a, b, $\cdots$ are obtained based on the Taylor expansion of Eq. (60) around the horizon. Now, because of Eq. (65) we can numerically explore the behavior of the conductivity for the $(1+1)$-dimensional holographic p-wave superconductor in the probe limit in the presence of BI nonlinear electrodynamics. Figures 5 and 6 give information about the behavior of the real and imaginary parts of conductivity as a function of ω/T for different values of nonlinearity parameter b in the case $\kappa^2 = 0$ for $T/T_c = 0.2, 0.5, 0.8$. The delta function in the real part of the conductivity is not related to the imaginary
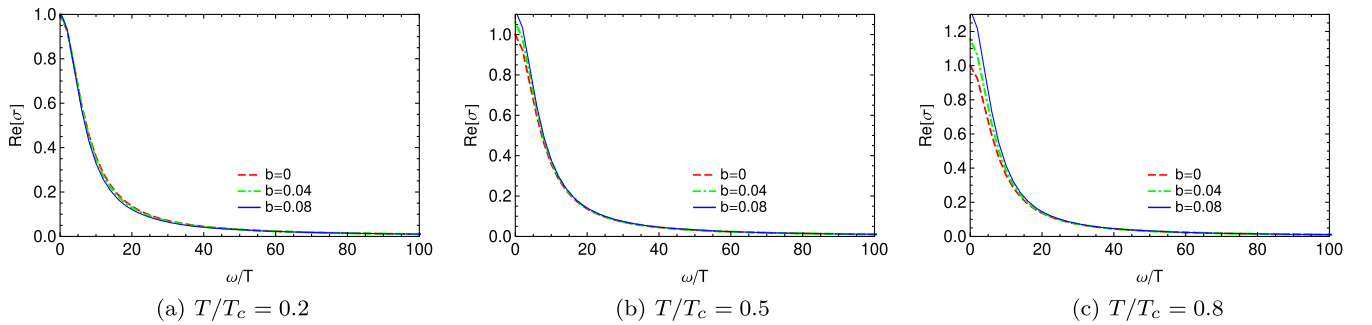
FIG. 7.   The behavior of the real part of the conductivity as a function of ω/T for different values of b in the case $\kappa^2 = 0$.
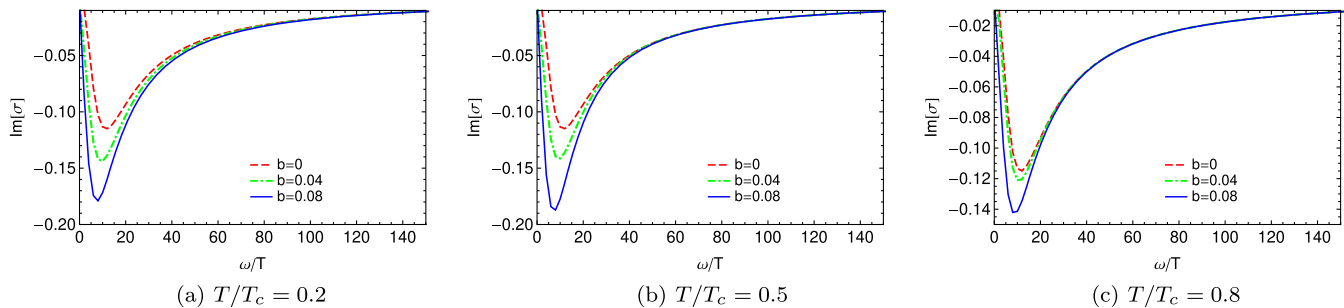
FIG. 8. The behavior of the imaginary part of the conductivity as a function of ω/T for different values of b in the case $\kappa^2 = 0$.

part near $\omega/T = 0$ by the Kramers-Kronig relation because the imaginary part tends to zero instead of having a pole in this region. In addition, $\text{Re}\sigma(\omega)$ tends to zero at high frequencies, as in [59]. The imaginary and real parts of conductivity follow a different trend in higher dimensions because we are faced with the absence of a gap and divergence behavior in the real and imaginary parts, respectively. Moreover, the effect of different values of temperature is more apparent for larger values of the nonlinearity parameter. Figures 7 and 8 show the effect of different values of the nonlinearity parameter b for fixed values of T/T_c. Based on these figures, the difference of the graphs becomes more obvious by increasing the value of T/T_c. In addition, for a fixed value of T/T_c, the effect of nonlinearity makes the Drude-like peak in the real part of the conductivity increase and causes deeper minimum values in the imaginary part.

VI. SUMMARY AND DISCUSSION

We have investigated the one-dimensional holographic p-wave superconductor model by applying AdS3/CFT2 when the gauge and vector fields backreact on the background geometry in the presence of BI nonlinear electrodynamics. For this purpose, we employ the Sturm-Liouville eigenvalue problem for analytical investigations and the shooting method for the numerical calculations. In both methods, we find the relation between the critical temperature T_c and the chemical potential μ for different values of the nonlinear and backreaction parameters. The results of analytical and numerical methods are in good agreement with each other. We found that increasing the values of the

nonlinearity and backreaction parameters decreases the critical temperature and thus makes it harder to form the condensation. Furthermore, the critical exponents of this system were also obtained both analytically and numerically. We are faced with a second order phase transition with $\beta = 1/2$ which follows the mean field theory. This value is independent of backreaction and nonlinear effects.

In addition, we analyzed the conductivity of this system for the case of the probe limit and investigated the properties of the real and imaginary parts of conductivity for different values of the nonlinear parameter b. The behavior of both the real and imaginary parts of conductivity are different from higher dimensions, and they do not connect to each other based on the Kramers-Kronig relation. We did not observe divergency near $\omega/T = 0$ in the imaginary part of the conductivity where a delta function in the real part appears. By increasing the effect of nonlinearity, we obtained larger values for a Drude-like peak in the real part of the conductivity and deeper minimum values of the imaginary part. It is difficult to see the effect of different temperatures for small values of the nonlinearity parameter. However, the effect of temperature becomes apparent by increasing b.

[1] S. A. Hartnoll, C. P. Herzog, and G. T. Horowitz, Phys. Rev. Lett. **101,** 031601 (2008).

[2] J. Bardeen, L. N. Cooper, and J. R. Schriefer, Phys. Rev. **108,** 1175 (1957).

[3] S. A. Hartnoll, Classical Quantum Gravity **26,** 224002 (2009).

[4] J. M. Maldacena, Adv. Theor. Math. Phys. **2,** 231 (1998).

[5] S. S. Gubser, I. R. Klebanov, and A. M. Polyakov, Phys. Lett. B **428,** 105 (1998).

[6] E. Witten, Adv. Theor. Math. Phys. **2,** 253 (1998).

[7] G. T. Horowitz and M. M. Roberts, Phys. Rev. D **78,** 126008 (2008).

[8] J. Ren, J. High Energy Phys. 11 (2010) 055.

[9] G. T. Horowitz, Lect. Notes Phys. **828**, 313 (2011).

[10] C. P. Herzog, J. Phys. A **42**, 343001 (2009).

[11] S. S. Gubser, C. P. Herzog, S. S. Pufu, and T. Tesileanu, Phys. Rev. Lett. **103**, 141601 (2009).

[12] S. A. Hartnoll, C. P. Herzog, and G. T. Horowitz, J. High Energy Phys. 12 (2008) 015.

[13] J. Jing and S. Chen, Phys. Lett. B **686**, 68 (2010).

[14] R. G. Cai, L. Li, L.-F. Li, and R.-Q. Yang, Sci China Phys. Mech. Astron. **58**, 1 (2015).

[15] X. H. Ge, B. Wang, S. F. Wu, and G. H. Yang, J. High Energy Phys. 08 (2010) 108.

[16] X. H. Ge, S. F. Tu, and B. Wang, J. High Energy Phys. 09 (2012) 088.

[17] X. M. Kuang, E. Papantonopoulos, G. Siopsis, and B. Wang, Phys. Rev. D **88**, 086008 (2013).

[18] Q. Pan, J. Jing, and B. Wang, J. High Energy Phys. 11 (2011) 088.

[19] R. G. Cai, H. F Li, and H. Q. Zhang, Phys. Rev. D **83**, 126007 (2011).

[20] R. G. Cai, Z. Y. Nie, and H. Q. Zhang, Phys. Rev. D **82**, 066007 (2010).

[21] W. Yao and J. Jing, J. High Energy Phys. 05 (2013) 101.

[22] S. Gangopadhyay and D. Roychowdhury, J. High Energy Phys. 05 (2012) 002; 05 (2012) 156.

[23] A. Sheykhi, D. H. Asl, and A. Dehyadegari, Phys. Lett. B **781**, 139 (2018).

[24] A. Sheykhi, A. Ghazanfari, and A. Dehyadegari, Eur. Phys. J. C **78**, 159 (2018).

[25] Z. Zhao, Q. Pan, S. Chen, and J. Jing, Nucl. Phys. **B871**, 98 (2013).

[26] Y. Liu, Y. Gong, and B. Wang, J. High Energy Phys. 02 (2016) 116.

[27] A. Sheykhi, H. R. Salahi, and A. Montakhab, J. High Energy Phys. 04 (2016) 058.

[28] H. R. Salahi, A. Sheykhi, and A. Montakhab, Eur. Phys. J. C **76**, 575 (2016).

[29] A. Sheykhi and F. Shaker, Int. J. Mod. Phys. D **26**, 1750050 (2017).

[30] A. Sheykhi and F. Shaker, Can. J. Phys. **94**, 1372 (2016).

[31] A. Sheykhi and F. Shaker, Phys. Lett. B **754**, 281 (2016).

[32] S. I. Kruglov, Ann. Phys. (Amsterdam) **530**, 1800070 (2018).

[33] B. B. Ghotbabadi, M. K. Zangeneh, and A. Sheykhi, Eur. Phys. J. C **78**, 381 (2018).

[34] M. Mohammadi, A. Sheykhi, and M. K. Zangeneh, Eur. Phys. J. C **78**, 654 (2018).

[35] M. Born and L. Infeld, Proc. R. Soc. A **144**, 425 (1934).

[36] S. H. Hendi and A. Sheykhi, Phys. Rev. D **88**, 044044 (2013).

[37] H. H. Soleng, Phys. Rev. D **52**, 6178 (1995).

[38] B. Hoffmann, Phys. Rev. **47**, 877 (1935).

[39] W. Heisenberg and H. Euler, Z. Phys. **98**, 714 (1936).

[40] H. P. de Oliveira, Classical Quantum Gravity **11**, 1469 (1994).

[41] G. W. Gibbons and D. A. Rasheed, Nucl. Phys. **B454**, 185 (1995).

[42] A. P. Mackenzie and Y. Maeno, Physica (Amsterdam) **280B**, 148 (2000).

[43] R.-G. Cai, S. He, L. Li, and L. F. Li, J. High Energy Phys. 12 (2013) 036.

[44] R. G. Cai, L. Li, and L. F. Li, J. High Energy Phys. 01 (2014) 032.

[45] A. Donos and J. P. Gauntlett, J. High Energy Phys. 12 (2011) 091.

[46] S. S. Gubser and S. S. Pufu, J. High Energy Phys. 11 (2008) 033.

[47] P. Chaturvedi and G. Sengupta, J. High Energy Phys. 04 (2015) 001.

[48] M. M. Roberts and S. A. Hartnoll, J. High Energy Phys. 08 (2008) 035.

[49] H. B. Zeng, W. M. Sun, and H. S. Zong, Phys. Rev. D **83**, 046010 (2011).

[50] R. G. Cai, Z. Y. Nie, and H. Q. Zhang, Phys. Rev. D **83**, 066013 (2011).

[51] L. A. P. Zayas and D. Reichmann, Phys. Rev. D **85**, 106012 (2012).

[52] D. Momeni, N. Majd, and R. Myrzakulov, Europhys. Lett. **97**, 61001 (2012).

[53] S. Gangopadhyay and D. Roychowdhury, J. High Energy Phys. 08 (2012) 104.

[54] S. Carlip, Classical Quantum Gravity **12**, 2853 (1995).

[55] A. Ashtekar, J. Wisniewski, and O. Dreyer, Adv. Theor. Math. Phys. **6**, 507 (2002).

[56] T. Sarkar, G. Sengupta, and B. N. Tiwari, J. High Energy Phys. 11 (2006) 015.

[57] E. Witten, Adv. Theor. Math. Phys. **2**, 505 (1998).

[58] S. Carlip, Classical Quantum Gravity **22**, R85 (2005).

[59] Y. Bu, Phys. Rev. D **86**, 106005 (2012).

[60] P. Chaturvedi and G. Sengupta, Phys. Rev. D **90**, 046002 (2014).

[61] R. Li, Mod. Phys. Lett. A **27**, 1250001 (2012).

[62] D. Momeni, M. Raza, M. R. Setare, and R. Myrzakulov, Int. J. Theor. Phys. **52**, 2773 (2013).

[63] Y. Peng and G. liu, Int. J. Mod. Phys. A **32**, 1750160 (2017).

[64] Y. Liu, Q. Pan, and B. Wang, Phys. Lett. B **702**, 94 (2011).

[65] N. Lashkari, J. High Energy Phys. 11 (2011) 104.

[66] H. B. Zeng, Phys. Rev. D **87**, 046009 (2013).

[67] Y. Bu, Phys. Rev. D **86**, 106005 (2012).

[68] Y. Peng, arXiv:1604.06990.

[69] M. Mohammadi, A. Sheykhi, and M. Kord Zangeneh, Eur. Phys. J. C **78**, 984 (2018).

[70] G. Alkac, S. Chakrabortty, and P. Chaturvedi, Phys. Rev. D **96**, 086001 (2017).

[71] D. Wen, H. Yu, Q. Pan, K. Lin, and W. L. Qian, Nucl. Phys. **B930**, 255 (2018).

[72] C. Lai, Q. Pan, J. Jing, and Y. Wang, Phys. Lett. B **749**, 437 (2015).